doi:10.1006/jmbi.2001.4509 available online at http://www.idealibrary.com on IDEAL® J. Mol. Biol. (2001) 307, 9–16

JMB

COMMUNICATION

Crystal Structure of Alginate Lyase A1-III Complexed with Trisaccharide Product at 2.0 Å Resolution

Hye-Jin Yoon, Wataru Hashimoto, Osamu Miyake, Kousaku Murata and Bunzo Mikami*

Research Institute for Food Science, Kyoto University, Uji Kyoto 611-0011, Japan

*Corresponding author

The structure of A1-III from a *Sphingomonas* species A1 complexed with a trisaccharide product (4-deoxy-L-*erythro*-hex-4-enepyranosyluronate-mannuronate-mannuronic acid) was determined by X-ray crystallography at 2.0 Å with an *R*-factor of 0.16. The final model of the complex form comprising 351 amino acid residues, 245 water molecules, one sulfate ion and one trisaccharide product exhibited a C^{α} r.m.s.d. value of 0.154 Å with the reported apo form of the enzyme. The trisaccharide was bound in the active cleft at subsites $-3 \sim -1$ from the non-reducing end by forming several hydrogen bonds and van der Waals interactions with protein atoms. The catalytic residue was estimated to be Tyr246, which existed between subsites −1 and +1 based on a mannuronic acid model oriented at subsite +1.

Keywords: alginate lyase; crystallization; X-ray crystallography; protein structure; enzyme-product complex

The *Sphingomonas* species A1 intracellularly produces three kinds of alginate lyase A1-I, -II and -III. Alginate lyase A1-I is believed to be autocatalytically processed to form A1-II and -III.[1] Though they are derived from the same gene product, the substrate specificities of the latter two lyases differ; that is, A1-II is an α-L-guluronosyl linkage-specific (G-G specific) lyase and preferentially acts on non-acetylated alginates produced by brown seaweed, whereas A1-III is a β-D-mannuronosyl linkage-specific (M-M specific) lyase and efficiently liquefies acetylated alginates produced by bacteria.[2] Among the ten families of polysaccharide lyase classified based on the sequence homology by Henrissat & Davies,[3] A1-III was classified to the family 5, but A1-II was classified as non-classified family. This finding supports the view that the two lyases have different structure and mechanisms of lyase action.[4] Alginate lyase A1-III consists of 364 amino acid residues with a molecular mass of 40 kDa. A1-III acts on alginate-tetrasaccharide as the minimum substrate and produces di- and trisaccharide from alginate.[2,4-6]

It has been suggested that the action of alginate lyase proceeds by the extraction of a hydrogen from a C-5 atom followed by the donation of a proton to the oxygen of the glycosidic bond to be cleaved, resulting in the formation of a product with a double bond between C-4 and C-5.[4,7,8] Though several authors assume that the histidine residue is a proton acceptor,[4,7] there is no direct evidence that the residue involves a catalytic step.

Among the ten families of polysaccharide lyase, the structures of the enzymes from family PE 1, PE 5, PE 7, and PE 8 have been determined. It is necessary to determine the structure of a complex of the enzyme with a substrate, inhibitor or product in order to identify important residues for catalysis. Recently, the complexes have been reported for a mutant pectate lyase C (family PE 1) with a plant cell wall fragment,[9] a chondroitinase B (family PE 6) with a disaccharide product[10] and a hyaluronate lyase (family PE 8) with a disaccharide product.[11]

We have determined the structure of the A1-III crystal at 1.78 Å resolution as a first report of a

Present address: H.-J. Yoon, Division of Chemistry and Molecular Engineering, Seoul National University, Seoul 151-742, Korea.

K.M. and B.M. contributed equally to this paper.

Abbreviations used: A1-III, alginate lyase A1-III; Hepes, *N*-(2-hydroxyethyl)piperazine-*N*′-(4-ethanesulfonic acid); r.m.s., root-mean-square; ΔM, 4-deoxy-α-L-*erythro*-hex-4-enepyranosyluronate; M, β-D-mannuronate.

E-mail address of the corresponding author: mikami@soya.food.kyoto-u.ac.jp

0022-2836/01/010009–8 $35.00/0

family PE 5 enzyme.[12] The three-dimensional structure of A1-III was abundant in helices and had a deep tunnel-like cleft in a novel (α_6/α_5)-barrel structure, which was similar to the (α_6/α_6)-barrel found in glucoamylase and cellulase. This structure presented the possibility that alginate molecules might penetrate into the cleft to interact with the catalytic site of A1-III. Though several residues important for the interaction with substrate were found in the presumed active site, without a bound substrate model catalytic residues have not been identified.

Here, in order to elucidate the catalytic site of A1-III, we describe the three-dimensional structure on of A1-III in complex with a trisaccharide product determined by X-ray crystallography at 2.0 Å resolution.

Structure determination

The diffraction data of a crystal of A1-III complexed with a trisaccharide product (4-deoxy-L-*erythro*-hex-4-enepyranosyluronate-mann-uronate-mannuronic acid; Figure 1) up to a 1.96 Å resolution was collected and refined to 2.0 Å resolution by X-PLOR[13] and CNS[14] using the model of refined A1-III (PDB, 1QAZ) determined previously.[12] Results of the X-ray data collection and refinement are summarized in Table 1.

The refined model of A1-III comprises 351 amino acid residues (residues from 4 to 354), 245 water molecules, one sulfate ion and one trisaccharide product. The stereo diagram of the ribbon representation of A1-III in complex with the trisaccharide product is shown in Figure 2(a). The N-terminal sequence from residue numbers 1 to 3 and the C-terminal sequence from 354 to 364 were not included in the present model because the $2|F_o| - |F_c|$ and $|F_o| - |F_c|$ maps were too weak to trace the correct sequence. The final overall *R*-factor for the refined model was 15.8 % (free *R*-factor, 19.8 %) using the data from 10.0 to 2.0 Å resolution (23,455 reflections). The final $2|F_o| - |F_c|$ map contoured at 1σ showed no discontinuity in the electron density of the main-chain, and in general, the electron density of the side-chains was very well defined. The final root-mean-square deviations from the standard geometry were 0.007 Å for bond lengths, 1.21° for bond angles, 21.03° for dihedral angles and 0.982° for improper angles.

Based on theoretical curves in the plot calculated by Luzzati,[15] the average positional standard deviation was estimated as close to 0.20 Å, between 5.0-2.0 Å resolution. Most of the residues fall in or near the energetically preferred regions in a Ramachandran plot[16] as they were observed in the native A1-III.[12]

Figure 2(b) shows an omit map of A1-III without the model of trisaccharide product. The difference Fourier map contoured at a 3σ level calculated with 10-2.0 Å resolution data had the highest

Table 1. Statistics of data collection and refinement of A1-III with complex

Crystal system	Monoclinic
Space group	*C*2
Unit cell (Å) β (deg.)	$a = 48.76$, $b = 92.92$, $c = 82.22$, $\beta = 104.11$
Molecules/asym. unit	1
V_m (Å^3/Da)	2.10
Data collection	
X-ray source	Cu-Kα
Detector	Bruker Hi-Star
Crystal-detector distance (cm)	15
Number of crystals used	1
Resolution limit (Å)	1.96
Scan width (deg.)	0.25
Scan rate (deg./minute)	0.25
Measured reflections	62,008
Unique reflections	23,455
Completeness ($\|I\| > 1\sigma\|I\|$, %)	92.5
R_{sym} (%)	5.2
Final model	351 residues, 245 water molecules, 1 sulfate ion, 1 trisaccharide
Resolution for refinement (Å)	10.0-2.0
Completeness ($\|F\| > 2\sigma\|F\|$, %)	87.5
Average *B*-factor Protein (Å^2)	22.67
Water (Å^2)	38.01
Sulfate (Å^2)	84.02
trisaccharide (Å^2)	39.23
R-factor (%)	15.8
R_{free} (%)	19.7
r.m.s.	
Bond lengths (Å)	0.007
Bond angles (deg.)	1.2
Dihedral angles (deg.)	21.0
Improper angles (deg.)	0.98

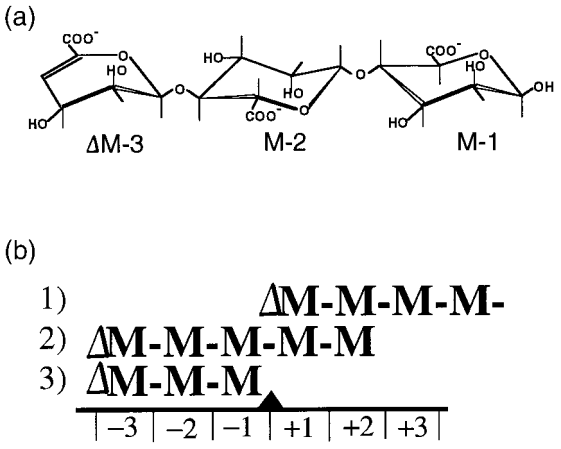

Figure 1. (a) The trisaccharide product (4-deoxy-L-*erythro*-hex-4-enepyranosyluronate-mannuronate-mannuronic acid). ΔM − 3, M − 2 and M − 1 designate 4-deoxy-L-*erythro*-hex-4-enepyranosyluronic acid at the non-reducing end and two mannuronic acid residues at the middle and reducing end, respectively. The trisaccharide product was prepared by gel filtration from the digest of the polymannuronate with alginate lyase A1-III as described Y.H.-J. *et al.*[6] (b) The binding mode of the products after: 1) first enzymatic attack, 2) final attack and 3) the possible binding mode of the trisaccharide product.

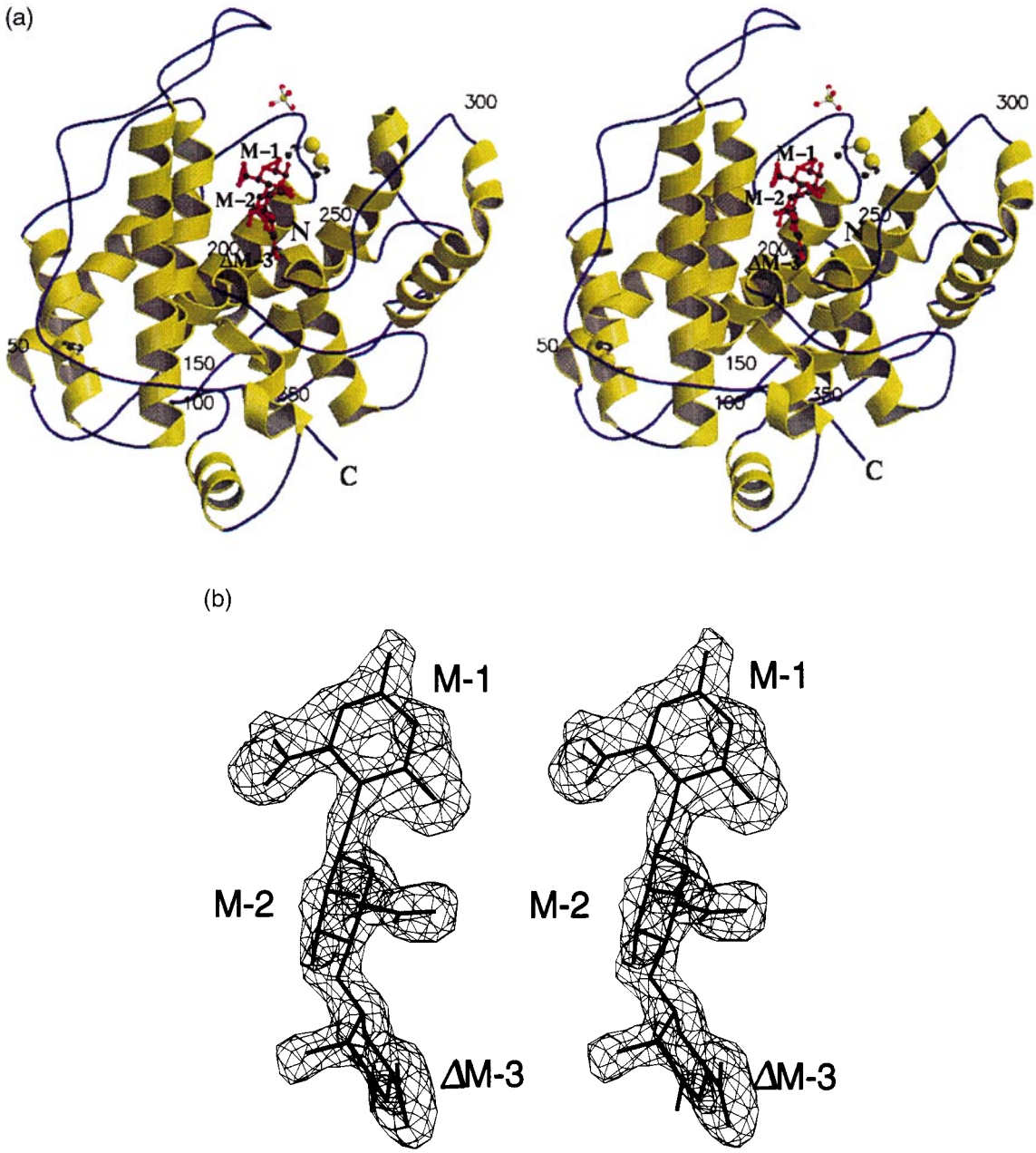

Figure 2. (a) Overall structure of the A1-III with trisaccharide product (ribbon stereo-diagram). The Figure shows loops (blue), 12 α-helices (yellow), one sulfate ion (green), and two S-S bridges, Cys49-Cys112, Cys188-Cys189 (yellow) and a trisaccharide product (red). The bound trisaccharide product, sulfate ions and the cystine residues are represented as ball-and-sticks. This figure was prepared using the programs MOLSCRIPT[19] and Raster3d.[20] (b) Stereo diagram of the omit map of A1-III without trisaccharide product. The omit map and trisaccharide molecule are shown as thin and thick lines. This Figure was prepared using the programs TURBO-FRODO (Bio-Graphics) on an Silicon Graphics INDY computer and Adobe Illustrator 5.5. Methods: A1-III was overexpressed in *Bacillus subtilis* and purified using a method described by Hisano *et al.*[1] The A1-III was crystallized by using the hanging-drop vapor-diffusion method in 0.1 M Hepes buffer (pH 7.5) conatining 48 % (w/v) saturated ammonium sulfate with a protein concentration of 8 mg/ml.[12] The crystals obtained were soaked in bottom solution containing 290 mM of the trisaccharide product of A1-III for one hour at 20 °C. The diffraction data of the A1-III crystal in complex with products up to 2.0 Å were collected with a Bruker Hi-Star multiwire area detector at 20 °C, using CuKα radiation generated by a MAC Science M18XHF rotating anode generator, and were processed with the SADIE and SAINT software packages (Bruker). The structure was refined by X-PLOR[13] and CNS[14] using the native A1-III model. Construct ion of the model was performed using the program TURBO-FRODO (Bio-Graphics) on an Silicon Graphics INDY computer. The stereo quality of the model was assessed using the programs PROCHECK[21] and WHAT-CHECK.[22]

densities in the trisaccharide region. The monosaccharide units of the product were designated as ΔM − 3, M − 2 and M − 1 from the non-reducing end according to the definition of Davies *et al*.[17] as shown in Figure 1. The displacement of the trisaccharide from the product position (subsites +1 ~ +3) to the observed position (subsites −3 ~ −1) is derived from the endo-type action of A1-III (Figure 1(b)). After the first cleavage the double-bonded non-reducing end should bind subsite less than −2, because the major product is known to be di- and triasaccharide.[2] The model of the trisaccharide product in the electron density was very well defined at M − 2 and M − 1 but slightly thin at ΔM − 3. The average *B*-factors for ΔM − 3, M − 2 and M − 1 were 44.5, 40.2 and 33.9 Å^2, respectively.

Carbohydrate-binding site

A1-III is composed of 12 α-helices that form a barrel structure with a deep tunnel-like cleft that is believed to be an active site. As anticipated, the trisaccharide product was positioned at the center of the deep cleft (Figure 2(a)). The configration of the trisaccharide was such that the non-reducing end (ΔM − 3, residue 401) was outside and the reducing end (M − 1, residue 403) was inside of the cleft. The bound trisaccharide product in the active site was in the $^4C_1$ -pyranosid forms except for the double-bonded sugar at the reducing end (Figure 2(b)). The torsion angles of the glycosidic bond defined as O-5′—C-1′—O-4—C-4 (ϕ) and C-1′—O-4—C-4—C-5 (ψ) between ΔM − 3 and M − 2 were −68.3° and −109.6°, and between M − 2 and M − 1 they were −63.3° and −177.2°, respectively. The β-anomer configurations were assigned to ΔM − 3-M − 2 and M − 2-M − 1. The trisaccharide molecule in the active site has been shown to have ϕ and ψ torsion angles in the lowest energy region of the isoenergy map.[18]

Figure 3(a) shows the bound trisaccharide molecule and the surrounding amino acid residues and water molecules interacting with the trisaccharide. The data listed in Table 2 represent the interactions of protein atoms with the bound trisaccharide molecule in the A1-III/trisaccharide complex. There are three and five direct hydrogen bonds between protein atoms and sugar residues of M − 2 and M − 1, respectively. N^{ε} and $N^{\eta 2}$ of Arg306 and $N^{\eta 2}$ of Arg312 form three hydrogen bonds with O-62 of M − 2. The side-chain O^{η} of Tyr246 forms two hydrogen bonds with O-1 and O-2 of M − 1. $N^{\varepsilon 2}$ of His245, $N^{\eta 2}$ of Arg88 and $N^{\eta 1}$ of Arg342 form three hydrogen bonds with O-3, O-62 and O-62 of M − 1, respectively. The carboxyl groups of M − 2 and M − 1 are therefore neutralized by Arg306 and Arg312, and by Arg88 and Arg 342, respectively. In contrast to M − 2 and M − 1, ΔM − 3 forms only one hydrogen bond between O-61 and the main-chain N of Gly313. The weak interaction of ΔM − 3 with protein groups implies that this trisaccharide product acts as a substrate analog based on the conformation of M − 2 and M − 1.

Besides the direct hydrogen bonds with protein atoms, M − 2 and M − 1 form nine and eight hydrogen bonds with surrounding water mol-

Table 2. Interactions between bound sugar atoms and protein atoms

Hydrogen bond			van der Waals contact	
Sugar atom	Protein atom	Distance (Å)	Sugar residue	Protein residue
ΔM − 3 O-61	Gly313 N	2.9		
M − 2 O-62	Arg306 N^{ε}	3.2	M−2	Arg306
M − 2 O-62	Arg306 $N^{\eta 2}$	3.0		
M − 2 O-62	Arg312 $N^{\eta 2}$	2.8		
M − 2 O-2	Wat634 O	2.6		
M − 2 O-2	Wat636 O	3.1		
M − 2 O-2	Wat635 O	3.0		
M − 2 O-3	Wat636 O	3.2		
M − 2 O-4	Wat688 O	3.2		
M − 2 O-5	Wat635 O	2.9		
M − 2 O-61	Wat744 O	2.5		
M − 2 O-62	Wat635 O	3.0		
M − 2 O-62	Wat744 O	3.1		
M − 1 O-1	Tyr246 O^{η}	3.2	M−1	Trp141
M − 1 O-2	Tyr246 O^{η}	3.1	M−1	Tyr246
M − 1 O-3	His245 $N^{\varepsilon 2}$	3.1	M−1	Tyr249
M − 1 O-62	Arg88 $N^{\eta 2}$	3.2		
M − 1 O-62	Arg342 $N^{\eta 1}$	3.0		
M − 1 O-1	Wat731 O	3.2		
M − 1 O-3	Wat635 O	2.8		
M − 1 O-4	Wat634 O	3.2		
M − 1 O-5	Wat641 O	2.9		
M − 1 O-61	Wat641 O	3.1		
M − 1 O-61	Wat655 O	2.8		
M − 1 O-61	Wat717 O	3.0		
M − 1 O-62	Wat640 O	2.9		

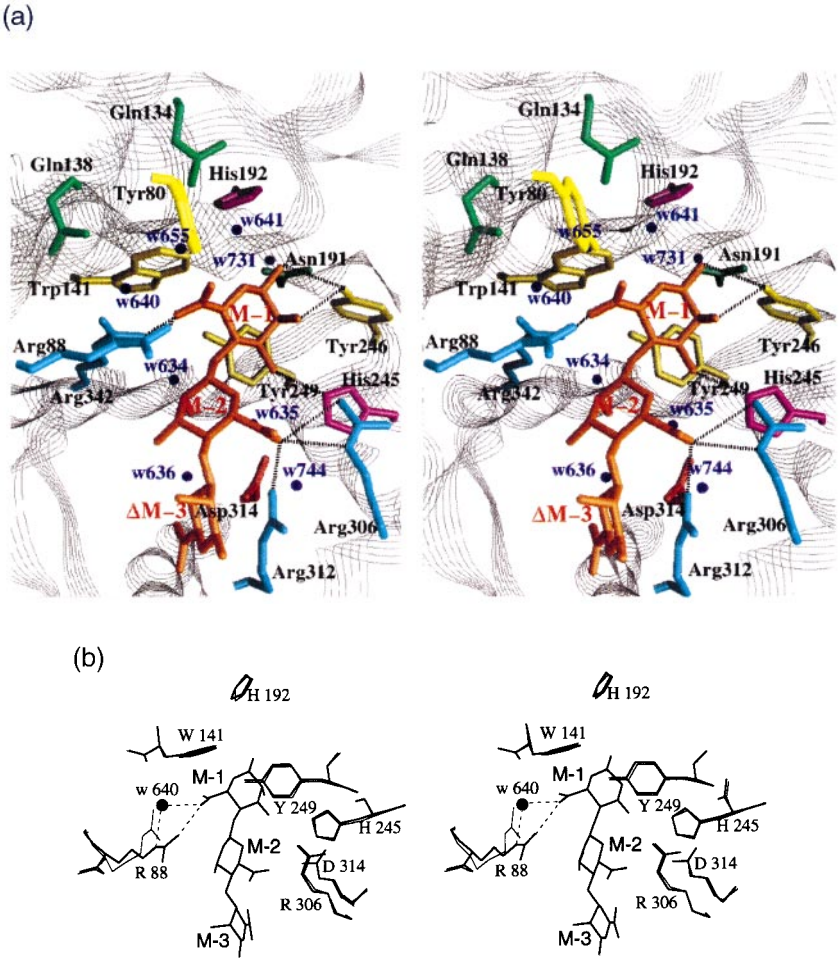

Figure 3. (a) The bound trisaccharide molecule on the active site of A1-III. The Figure shows the bound trisaccharide molecule and the surrounding amino acid residues and water molecules interacting with the trisaccharide. The trisaccharide molecule is represented by means of an orange ball-and-stick model. The side-chains of Tyr and Trp, Asn and Gln, Asp, Arg, and His residues are colored yellow, green, red, cyan and purple, respectively. The water molecules are shown as a filled circle (●). The hydrogen bonds between trisaccharide and protein residues or water molecules less than 3.25 Å are shown as dotted lines. This Figure was drawn using the program GRASP.[23] (b) The conformational change of A1-III induced by the binding of trisaccharide products. A1-III and A1-III with trisaccharide structures are represented as thin and thick lines, respectively. The water molecules are shown as a filled circle (●). The hydrogen bonds in trisaccharide, protein residues or water molecules less than 3.25 Å are shown as dotted lines. This Figure was prepared using the programs TURBO-FRODO (Bio-Graphics) on a Silicon Graphics INDY computer and Adobe Illustrator 5.5.

ecules, respectively. There are five water-mediated hydrogen bonds between M − 2 and protein residues: O 2 . . . Wat634 . . . Tyr249 O (2.8 Å), O 2 . . . Wat634 . . . Arg342 $N^{\eta 1}$ (2.9 Å), O 2 . . . Wat635 . . . Asp314 $O^{\delta -1}$ (2.7 Å), O 2 . . . Wat636 . . . Asp314 $O^{\delta 2}$ (3.1 Å) and O 61 (O 62) . . . Wat744 . . . Arg312 $N^{\eta 1}$ (2.9 Å). Ten water-mediated hydrogen bonds are also found between M − 1 and protein residues: O-1 . . . Wat731 . . . Asn191 $O^{\delta 1}$ (2.9 Å), O-1 . . . Wat731 . . . His 192 $N^{\varepsilon 2}$ (3.2 Å), O-3 . . . Wat635 . . . Asp314 $O^{\delta 2}$ (3.1 Å), O-5 (O-61) . . . Wat641 . . . Gln134 $O^{\varepsilon 1}$ (3.0 Å), O-62 . . . Wat640 . . . Arg88 $N^{\eta 2}$ (3.1 Å), O-62 . . . Wat640 . . . Arg88 $N^{\eta 2}$ (2.9 Å), O-62 . . . Wat640 . . . Arg88 N^{ε} (3.1 Å), O-61 . . . Wat655 . . . Tyr80 O (2.9 Å), O-62 . . . Wat640 . . . Gln138 $N^{\varepsilon 2}$ (3.1 Å) and O-62 . . . Wat640 . . . Arg342 $N^{\eta 2}$ (2.9 Å). In contrast to the abundance of hydrogen bonds, a few van der Waals contacts were found between the side-chain of Arg306 and M − 2, and between the side-chains of Trp141, Tyr246 and Tyr249 and M − 1 (Table 2). Tyr 249 forms a partially stacked interaction with a sugar ring of M − 2 with a distance of 3.4 Å between C^{ζ} and C-3. There are vacant spaces around O-2 and O-3 of ΔM − 3 and M − 2 and around O-2 of M − 1, which can accommodate acetyl groups in accordance with the specificity of this enzyme.

Conformational changes of A1-III induced by trisaccharide

Figure 3(b) shows the conformational changes of A1-III induced by the binding of the trisaccharide

products. A1-III and A1-III complexed with the trisaccharide were superimposed by a fitting program implemented in TURBO-FRODO (Bio-Graphics). The r.m.s.d. value was 0.154 Å for 351 common C^{α} atoms. The trisaccharide molecules replaced five water molecules present in the active site of A1-III. No significant conformational change was found in the protein structure except for in the side-chain of Arg88. C^{ζ} of Arg88 migrated 2.2 Å toward the COOH group of M − 1, while its C^{α} moved only 0.36 Å. The water 640 located near the Arg88 $N^{\eta 2}$ of native A1-III played an important role in water-mediated hydrogen bonds between M − 1 O-62 and Arg88 $N^{\eta 2}$ and between M − 1 O-62 and Gln138 $N^{\varepsilon 2}$.

Possible catalytic mechanism of A1-III

The catalytic site of A1-III should be located between subsites −1 and +1 as estimated from the native A1-III structure.[12] The M + 1 mannouronic acid residue was manually constructed from the M − 1 residue by a small adjustment of the ϕ and j torsion angles. Figure 4(a) shows the constructed model of M + 1 together with M − 1 and the surrounding protein residues. The (ϕ, ψ) torsion angles between M − 1 and M + 1, found to be −78.3° and −149.1°, respectively, are in the lowest energy region.[18] The carboxyl groups of M + 1 can interact with the side-chain of Arg239 and possibly with that of Asn191, and O-5 can interact with the side-chain of His192, which is located at the opposite side of a hydrogen of the C-5 atom. In this model, His192 cannot act as a base to extract a hydrogen from the C-5 atom. It is most likely that the base is Tyr246, which is located near the O-1 and O-2 of M − 1 (Table 2). The negative charge of ionized Tyr246 is stabilized by the positive charge of Arg239 because the distance between the O^{η} of Tyr246 and the $N^{\eta 2}$ of Arg239 is only 3.5 Å. The distance between the O^{η} of Tyr246 and the C-5 of M + 1 was estimated to be 3.6 Å based on the model. The ionized Tyr246 can extract the hydrogen from C-5 and it can also act as a hydrogen donor to the oxygen of the glycosidic linkage to be cleaved. Figure 4(b) shows the predicted mechanism of A1-III action. The reaction follows the mechanism of lyase specific for the substrate with an axial-equatorial relationship as proposed by Linhardt *et al.*[3,4] except that the base residue and the

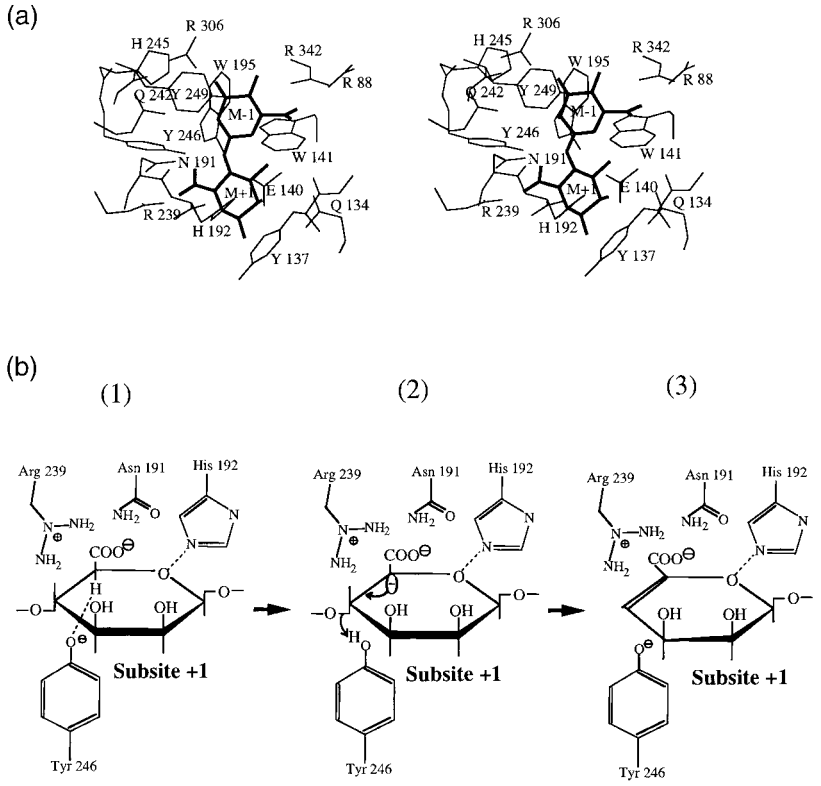

Figure 4. (a) Stereo diagram showing the spatial orientation of M − 1, reducing end of the bound trisaccharide product with manually constructed M + 1 in the catalytic site of A1-III. (b) Schematic representation of polymannuronic acid degradation mechanism. (1) Arg239 interacts with the carboxyl group of M + 1 and with Tyr246 to stabilize the negative charge of the ionized side-chain. His192 is hydrogen-bonded to O-5 of the sugar. Tyr246 is positioned close to O-4 and C-5. (2) Tyr246 extracts the proton of C-5, resulting in the formation of a carboxylate dianion intermediate. (3) Tyr246 donates a proton to the glycosidic oxygen, resulting in the cleavage of the glycosidic bond and the formation of a double bond between the C-4 and C-5 atoms.

proton donor is the same Tyr residue. First, the negative charge on the C-5 carboxylate group is neutralized by Arg239 and Asn191. Subsequently, the C-5 proton can more easily be removed and in the next step, Tyr246 extracts a proton from C-5 of the mannuronic acid, resulting in the formation of a carboxylate dianion intermediate. It seems inevitable that His192 stabilizes the intermediate. Then, Tyr246 donates a proton to the oxygen of the glycosidic bond, resulting in the formation of a double bond between C-4 and C-5 and the cleavage of the glycosidic bond. Our hypothesis that the side-chain of Tyr acts as both a proton acceptor and donor is quite different from previously reported ideas concerning the mechanism of polysaccharide lyases. Greiling *et al*. proposed that the mechanism of hyaluronate lyase action was based on a single histidine residue which could act successively as a proton acceptor and proton donor.[7] Gacesa also proposed a three-step mechanism of alginate lyase.[8] Based on a manually reoriented substrate model of hyaluronate lyase determined by X-ray crystallographic analysis, Ponnuraj *et al*.[11] proposed a mechanism involving three residues His399, Tyr408 and Asn349, in which His399 and Tyr408 act as a proton acceptor and a proton donor, respectively. These authors assume that His residues act as a proton acceptor. Our hypothesis that Tyr246 acts as a proton acceptor and a proton doner is based on the structure of an extended mannuronic acid residue from a bound trisaccharide. In order to prove the present hypothesis, we are now trying to construct the mutants of A1-III in which Tyr246 and His192 are converted to Phe246 and Ala192, respectively. The structural analysis of the mutant enzymes/substrate complex will clarify the details of the mechanism of this enzyme.

Protein Data Bank accession codes

Coordinates of the A1-III with the trisaccharide product have been deposited in the RCSB Protein Data Bank operated by Research Collaboratory for Structural Bioinformatics under the accession number 1HV6.

Acknowledgments

Computation time was provided by the Supercomputer Laboratory, Institute for Chemical Research, Kyoto University. This work was supported, in part, by a Grant-in-Aid for Scientific Research from the Ministry of Education, Science and Culture of Japan.

References

1. Hisano, T., Nishimura, M., Yamashita, T., Sakaguchi, K. & Murata, K. (1994). On the self-processing of bacterial alginate lyase. *J. Ferment. Bioeng.* **78**, 109-110.
2. Murata, K., Inose, T., Hisano, T., Abe, S., Yonemoto, Y., Yamashita, T., Takagi, M., Sakaguchi, K., Kimura, A. & Imanaka, T. (1993). Bacterial alginate lyase: enzymology, genetics and application. *J. Ferment. Bioeng.* **76**, 427-437.
3. Henrissat, B. & Davies, G. J. (1997). Structural and sequence-based classification of glycoside hydrolases. *Curr. Opin. Struct. Biol.* **7**, 637-644.
4. Linhardt, R. J., Galliher, P. M. & Cooney, C. L. (1986). Polysaccharide lyases. *Appl. Biochem. Biotechnol.* **12**, 135-176.
5. Yonemoto, Y., Tanaka, H., Hisano, T., Sakaguchi, K., Abe, S., Yamashita, T., Kimura, A. & Murata, K. (1993). Bacterial alginate lyase gene: nucleotide sequence and molecular route for the generation of alginate lyase species. *J. Ferment. Bioeng.* **75**, 336-342.
6. Yoon, H.-J., Hashimoto, W., Miyake, O., Okamoto, M., Mikami, B. & Murata, K. (2000). Overexpression in *Escherichia coli*, purification, and characterization of *Sphingomonas* sp. A1 alginate lyases. *Protein Expr. Purif.* **19**, 84-90.
7. Greiling, H., Stuhlsatz, H. W., Eberhard, T. & Eberhard, A. (1975). Studies on the mechanism of hyaluronate lyase action. *Connect. Tissue Res.* **3**, 135-139.
8. Gacesa, P. (1987). Alginate-modifying enzymes. A proposed unified mechanism of action for the lyases and epimerases. *FEBS Letters,* **212**, 199-202.
9. Scavetta, R. D., Herron, S. R., Hotchkiss, A. T., Kita, N., Keen, N. T., Benen, J. A. *et al*. (1999). Structure of a plant cell wall fragment complexed to pectate lyase C. *Plant Cell,* **11**, 1081-1092.
10. Huang, W., Matte, A., Li, Y., Kim, Y. S., Linhardt, R. J., Su, H. & Cygler, M. (1999). Crystal structure of chondroitinase B from *Flavobacterium heparinum* and its complex with a disaccharide product at 1.7 Å resolution. *J. Mol. Biol.* **294**, 1257-1269.
11. Ponnuraj, K. & Jedrzejas, M. J. (2000). Mechanism of hyaluronan binding and degradation structure of *Streptococcus pneumoniae* hyaluronate lyase in complex with hyaluronic acid disaccharide at 1.7 Å resolution. *J. Mol. Biol.* **299**, 885-895.
12. Yoon, H.-J., Mikami, B., Hashimoto, W. & Murata, K. (1999). Crystal structure of alginate lyase A1-III from *Sphingomonas* species A1 at 1.78 Å resolution. *J. Mol. Biol.* **290**, 505-514.
13. Brünger, A. T. (1992). *X-PLOR Version 3.1 Manual: A System for Crystallography and NMR*, Yale University, New Haven, CT.
14. Brünger, A. T., Adams, P. D., Clore, G. M., DeLano, W. L., Gros, P., Grosse-Kunstleve, R. W. *et al*., (1998). Crystallography and NMR system (CNS): a new software system for macromolecular structure determination. *Acta Crystallog. sect. D,* **54**, 905-921.
15. Luzzati, V. (1952). Traitement statistique des erreurs dans la determination des structures cristallines. *Acta. Crystallog.* **5**, 802-810.
16. Ramachandran, G. N. & Sasisekharan, V. (1968). Conformations of polypeptides and proteins. *Advan. Protein Chem.* **23**, 283-437.
17. Davies, G. J., Wilson, K. S. & Henrissat, B. (1997). Nomenclature for sugar-binding subsites in glycosyl hydrolases. *Biochem. J.* **15**, 557-559.
18. Braccini, I., Grasso, R. P. & Perez, S. (1999). Conformational and configurational features of acidic polysaccharides and their interactions with calcium ions: a molecular modeling investigation. *Carbohydrate Res.* **317**, 119-130.

19. Kraulis, P. J. (1991). MOLSCRIPT: a program to produce both detailed and schematic plots of protein structure. *J. Appl. Crystallog.* **24**, 946-950.
20. Merrit, E. A. & Murphy, M. E. P. (1994). RASTER3D Version 2.0. A program for photorealistic molecular graphics. *Acta Crystallog. sect. D,* **50**, 869-873.
21. Laskowski, R. A., MacArthur, M. W., Moss, D. S. & Thornton, J. M. (1993). PROCHECK: a program to check the stereochemical quality of protein structures. *J. Appl. Crystallog.* **26**, 283-291.
22. Hooft, R. W., Vriend, G., Sander, C. & Abola, E. E. (1996). Errors in protein structures. *Nature,* **381**, 272.
23. Nicholls, A., Sharp, K. & Honig, B. (1991). Protein folding and association: insights from the interfacial and thermodynamic properties of hydrocarbons. *Proteins: Struct. Funct. Genet.* **11**, 281-296.

Edited by R. Huber

(Received 10 October 2000; received in revised form 19 January 2001; accepted 19 January 2001)